IEEE Access
Multidisciplinary | Rapid Review | Open Access Journal

Received October 11, 2020, accepted November 3, 2020, date of publication November 19, 2020, date of current version December 7, 2020.

*Digital Object Identifier 10.1109/ACCESS.2020.3038830*

# Design of Three-Dimensional Guidance Law With Impact Angle Constraints and Input Saturation

**TONG LI AND HUAMING QIAN**
College of Intelligent Systems Science and Engineering, Harbin Engineering University, Harbin 150001, China
Corresponding author: Huaming Qian (qianhuam@sina.com)

This work was supported by the National Natural Science Foundation of China under Grant 61573113.

**ABSTRACT** This thesis studies the problem of three-dimensional guidance considering maneuvering acceleration and input saturation based on the background of missile intercepting maneuvering target. On the basis of the three-dimensional guidance model with impact angle constraints, a three-dimensional guidance law is designed by using the integral sliding mode control and adaptive control. To solve the problem of input saturation, an adaptive anti-saturation integral sliding mode three-dimensional guidance law is designed by introducing an auxiliary system. The stability of the designed guidance law is proved by Lyapunov theory, which ensures that the sliding mode manifold converges to zero in finite time. The effectiveness of the designed guidance law is verified by simulation analysis.

**INDEX TERMS** Three-dimensional guidance law, input saturation, integral sliding mode control, adaptive control.

## I. INTRODUCTION

With the complexity of the war environment and the increasing improvement of the performance of high maneuvering targets, the missile must have the ability to intercept air maneuvering targets [1]. The design of robust three-dimensional guidance law is the key link to ensure the successful interception of the target. In order to achieve the best damage effect, the missile is usually required to intercept the target at the desired impact angle [2]. Therefore, it is of great significance to study the three-dimensional guidance law with impact angle constraints.

Among the common guidance law design methods in automatic seeking guidance system, the main methods include classical control methods and modern control methods. In [3], [4], a bias pure proportional guidance law is designed for intercepting stationary or slow targets. In order to achieve the best damage effect, a proportional guidance law with angle constraint is designed for the relative motion model of three-dimensional missile and target [5], [6]. In [7], [8], the guidance law with impact angle constraint is designed based on the optimal control theory. Because the sliding mode guidance law is robust to external disturbances and the uncertainty of system parameters, it has been widely used in aircraft guidance and control [9]–[15]. In [10], [11], based on the sliding mode control, an adaptive guidance law with impact angle constraints is designed. In order to obtain high precision guidance performance, the finite-time guidance law is designed by using the terminal sliding mode control in [12], [13]. In [14], the sliding mode three-dimensional guidance laws with impact angle constraints are designed for maneuvering target interception. In [15], a robust guidance law with impact angle constraints is designed for intercepting maneuvering targets based on the adaptive control and nonsingular terminal sliding mode control. In [16], the nonlinear disturbance observer is used to estimate the target acceleration on line, and the three-dimensional guidance law is designed by using the finite-time control. In the actual guidance process, the acceleration command of the missile has certain physical constraints. If the acceleration instruction constraint is not considered in the design of the guidance law, it may lead to the decline of the guidance performance and even cause the instability of the whole guidance system in [17]. In [18], [19], based on the adaptive control and optimal control, the adaptive three-dimensional guidance law and the optimal guidance law with input saturation constraints are designed. In [20], an anti-saturation three-dimensional guidance law with impact angle constraints is designed. In [21], to deal with the problem of input saturation, an adaptive dynamic surface three-dimensional guidance law is designed

The associate editor coordinating the review of this manuscript and approving it for publication was Haibin Sun.

by using the smooth tangent function and Nussbaum function. In [22], [23], by introducing an adaptive algorithm to estimate the upper bound of target acceleration online, a three-dimensional guidance law with acceleration constraint is designed by using the dynamic control, but the state of the guidance system can only be guaranteed to be uniformly bounded. In order to further improve the interception probability for high maneuvering targets, in this paper, a 3D guidance strategy with impact angle constraints is designed based on the integral terminal sliding mode theory and adaptive algorithm. Compared with the above references, the innovations are as follows

(1) By designing the integral terminal sliding mode surface with adaptive gain and automatically adjusting the adaptive gain parameters according to the error information, the system error converges to the sliding mode surface quickly and the control performance of the system is improved.

(2) In this paper, the adaptive terminal sliding mode controller and anti-saturation adaptive terminal controller are designed respectively, so that the state of the system converges to the equilibrium point quickly in finite time.

(3) Compared with [15], this paper considers input saturation and finite-time stability, which is of more practical engineering significance.

The structures of this paper are as follows: Firstly, the guidance model of three-dimensional space with impact angle constraints is given. Secondly, based on the integral terminal sliding mode control theory and adaptive control method, the adaptive integral terminal sliding mode guidance law and the anti-saturation adaptive integral terminal sliding mode guidance law are designed respectively. Finally, the effectiveness of the designed guidance law is verified by digital simulation.

## II. SYSTEM DYNAMICS AND PROBLEM STATEMENT

Fig. 1 shows the three-dimensional guidance geometry of the missile intercepting the maneuvering target. The relative kinematic equation of the missile and target is given as follows [13]

$$\dot{R} = (\rho\cos\theta_t\cos\phi_t - \cos\theta_m\cos\phi_m)V_m \tag{1}$$

$$R\dot{\theta}_L = (\rho\sin\theta_t - \sin\theta_m)V_m \tag{2}$$

$$\dot{\phi}_L R\cos\theta_L = (\rho\cos\theta_t\sin\phi_t - \cos\theta_m\sin\phi_m)V_m \tag{3}$$

$$\dot{\theta}_m = \frac{a_{zm}}{V_m} - \dot{\phi}_L\sin\theta_L\sin\phi_m - \dot{\theta}_L\cos\phi_m \tag{4}$$

$$\dot{\phi}_m = \frac{a_{ym}}{V_m\cos\theta_m} + \dot{\phi}_L\sin\theta_L\cos\phi_m\tan\theta_m - \dot{\theta}_L\sin\phi_m\tan\theta_m - \dot{\phi}_L\cos\theta_L \tag{5}$$

$$\dot{\theta}_t = \frac{a_{zt}}{\rho V_m} - \dot{\phi}_L\sin\theta_L\sin\phi_t - \dot{\theta}_L\cos\phi_t \tag{6}$$

$$\dot{\phi}_t = \frac{a_{yt}}{\rho V_m\cos\theta_t} + \dot{\phi}_L\sin\theta_L\cos\phi_t\tan\theta_t - \dot{\theta}_L\sin\phi_t\tan\theta_t - \dot{\phi}_L\cos\theta_L \tag{7}$$

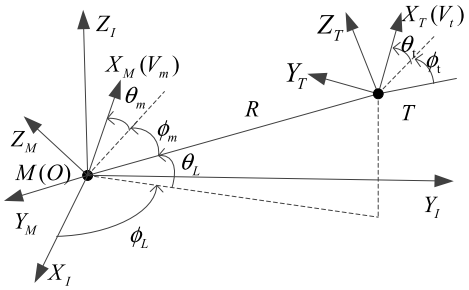


**FIGURE 1.** Geometry in a three-dimensional space.

where $\rho = V_t/V_m$, $V_m$ and $V_t$ are the missile velocity and target velocity, respectively. $R$ is the relative distance. $\theta_m$ and $\phi_m$ represent the direction of the velocity of the missile relative to the line-of-sight. $\theta_t$ and $\phi_t$ represent the direction of the velocity of the target relative to the line-of-sight coordinate system. $\theta_L$ and $\phi_L$ are the angles of sight. $a_{ym}$ and $a_{zm}$ are the missile accelerations in the pitch and yaw directions. $a_{yt}$ and $a_{zt}$ are the target accelerations in the pitch and yaw directions, respectively.

Based on (5) and (7), the following equation holds

$$\ddot{\theta}_L = \frac{\cos\theta_t}{R}a_{zt} - \frac{\cos\theta_m}{R}a_{zm} - \dot{\phi}_L^2\cos\theta_L\sin\theta_L - \frac{2\dot{R}\dot{\theta}_L}{R} \tag{8}$$

$$\ddot{\phi}_L = \frac{\cos\phi_t}{R\cos\theta_L}a_{yt} - \frac{\sin\theta_t\sin\phi_t}{R\cos\theta_L}a_{zt} + \frac{\sin\theta_m\sin\phi_m}{R\cos\theta_L}a_{zm} - \frac{\cos\phi_m}{R\cos\theta_L}a_{ym} + 2\dot{\phi}_L\dot{\theta}_L\tan\theta_L - \frac{2\dot{R}\dot{\phi}_L}{R} \tag{9}$$

Let $\boldsymbol{x} = \begin{bmatrix} x_1 \\ x_2 \end{bmatrix} = \begin{bmatrix} \theta_L \\ \phi_L \end{bmatrix}$, combining (8) and (9), the three-dimensional guidance system described as

$$\ddot{\boldsymbol{x}} = \boldsymbol{F} + \boldsymbol{B}\boldsymbol{u} + \boldsymbol{D} \tag{10}$$

where $\boldsymbol{u}$ is control input, $\boldsymbol{D}$ is external disturbances, in the following form

$$\boldsymbol{F} = \begin{bmatrix} -\dot{\phi}_L^2\cos\theta_L\sin\theta_L - \dfrac{2\dot{R}\dot{\theta}_L}{R} \\ 2\dot{\phi}_L\dot{\theta}_L\tan\theta_L - \dfrac{2\dot{R}\dot{\phi}_L}{R} \end{bmatrix},$$

$$\boldsymbol{D} = \begin{bmatrix} \dfrac{\cos\theta_t}{R}a_{zt} \\ \dfrac{\cos\phi_t}{R\cos\theta_L}a_{yt} - \dfrac{\sin\theta_t\sin\phi_t}{R\cos\theta_L}a_{zt} \end{bmatrix},$$

$$\boldsymbol{B} = \begin{bmatrix} -\dfrac{\cos\theta_m}{R} & 0 \\ \dfrac{\sin\theta_m\sin\phi_m}{R\cos\theta_L} & -\dfrac{\cos\phi_m}{R\cos\theta_L} \end{bmatrix}, \boldsymbol{u} = \begin{bmatrix} a_{zm} \\ a_{ym} \end{bmatrix}.$$

To facilitate the terminal guidance law design, the following lemma and assumption are given.

*Assumption 1:* Considering the system (10), assume that the external disturbances $\boldsymbol{D}$ is bounded, that is $\|\boldsymbol{D}\| \leq D$, where $D$ is positive constant.

*Lemma 1* [13]: Considering system $\dot{\boldsymbol{x}} = f(\boldsymbol{x}, t), \boldsymbol{x} \in \boldsymbol{R}^n$, suppose $V(x)$ is a $C^1$ smooth positive definite function (defined on $U \subset R^n$) and $\dot{V}(x) + \zeta V^{\delta}(x)$ is negative semi-definite on $U \subset R^n$ for $\delta \in (0, 1)$ and $\zeta \in R^+$,then there exists an area $U_0 \subset R^n$ such that any $V(x)$ which stars from $U_0 \subset R^n$ can reach $V(x) \equiv 0$ in finite time. Moreover, if $T_r$ is the time needed to reach $V(x) \equiv 0$, then $T_r \leq \frac{V^{1-\delta}(x_0)}{\zeta(1-\delta)}$, where $V(x_0)$ is the initial value of $V(x)$.

*Lemma 2* [9]: Consider the following $n$ order integral system

$$\dot{x}_1 = x_2, \cdots, \dot{x}_{n-1} = x_n, \dot{x}_n = u \tag{11}$$

If $\varepsilon \in (0, 1)$ that satisfies for any $\alpha_n \in (1 - \varepsilon, 1)$, and the design controller is

$$u = -k_1 sig^{\alpha_1}(x_1) - k_2 sig^{\alpha_2}(x_2) - \cdots - k_n sig^{\alpha_n}(x_n) \tag{12}$$

where $\alpha_1, \alpha_2, \cdots, \alpha_n$ satisfies $\alpha_{i-1} = \frac{\alpha_i \alpha_{i+1}}{2\alpha_{i+1} - \alpha_i}, i = 2, 3, \cdots, n, \alpha_{n+1} = 1$. $\lambda^n + k_n\lambda^{n-1} + \cdots + k_2\lambda + k_1$ is the polynomial of Hurwitz. Then, the system is globally finite time stable.

## III. GUIDANCE LAW DESIGN

Based on the integral terminal sliding mode control and adaptive algorithm, the adaptive guidance law and anti-saturation guidance law are designed for the three-dimensional guidance system (10), respectively, to ensure the missile to intercept the maneuvering target successfully.

### A. DESIGN OF ADAPTIVE INTERTAL SLIDING MODE CONTROLLER

The integral sliding mode surface is defined as follows

$$\begin{aligned} \boldsymbol{s} &= \begin{bmatrix} s_1 \\ s_2 \end{bmatrix} \\ &= \begin{bmatrix} \dot{x}_1 - \dot{x}_1(0) + \hat{\Lambda}_1 \int_0^t (k_1 \mathrm{sig}^{\alpha_1}(x_1) + k_2 \mathrm{sig}^{\alpha_2}(\dot{x}_1))\mathrm{d}t \\ \dot{x}_2 - \dot{x}_2(0) + \hat{\Lambda}_2 \int_0^t (l_1 \mathrm{sig}^{\beta_1}(x_2) + l_2 \mathrm{sig}^{\beta_2}(\dot{x}_2))\mathrm{d}t \end{bmatrix} \end{aligned} \tag{13}$$

where $k_1, k_2, l_1$ and $l_2$ are positive constants, $0 < \alpha_1 < 1, 0 < \alpha_2 < 1, 0 < \beta_1 < 1, 0 < \beta_2 < 1, \hat{\Lambda}_1$ and $\hat{\Lambda}_2$ are the adaptive gains.

Computing the derivative of $\boldsymbol{s}$, it can obtained as

$$\begin{aligned} \dot{\boldsymbol{s}} &= \begin{bmatrix} \dot{s}_1 \\ \dot{s}_2 \end{bmatrix} = \begin{bmatrix} \ddot{x}_1 + \dot{\hat{\Lambda}}_1 \int_0^t (k_1 \mathrm{sig}^{\alpha_1}(x_1) + k_2 \mathrm{sig}^{\alpha_2}(\dot{x}_1))\mathrm{d}t \\ +\hat{\Lambda}_1 (k_1 \mathrm{sig}^{\alpha_1}(x_1) + k_2 \mathrm{sig}^{\alpha_2}(\dot{x}_1)) \\ \ddot{x}_2 + \dot{\hat{\Lambda}}_2 \int_0^t (l_1 \mathrm{sig}^{\beta_1}(x_2) + l_2 \mathrm{sig}^{\beta_2}(\dot{x}_2))\mathrm{d}t \\ +\hat{\Lambda}_2 (l_1 \mathrm{sig}^{\beta_1}(x_2) + l_2 \mathrm{sig}^{\beta_2}(\dot{x}_2)) \end{bmatrix} \\ &= \boldsymbol{F} + \boldsymbol{B}\boldsymbol{u} + \boldsymbol{D} + \boldsymbol{M} \\ &\quad + \begin{bmatrix} \dot{\hat{\Lambda}}_1 \int_0^t (k_1 \mathrm{sig}^{\alpha_1}(x_1) + k_2 \mathrm{sig}^{\alpha_2}(\dot{x}_1))\mathrm{d}t \\ \dot{\hat{\Lambda}}_2 \int_0^t (l_1 \mathrm{sig}^{\beta_1}(x_2) + l_2 \mathrm{sig}^{\beta_2}(\dot{x}_2))\mathrm{d}t \end{bmatrix} \end{aligned} \tag{14}$$

where $\boldsymbol{M} = \begin{bmatrix} k_1 \hat{\Lambda}_1 \mathrm{sig}^{\alpha_1}(x_1) + k_2 \hat{\Lambda}_1 \mathrm{sig}^{\alpha_2}(\dot{x}_1) \\ l_1 \hat{\Lambda}_2 \mathrm{sig}^{\beta_1}(x_2) + l_2 \hat{\Lambda}_2 \mathrm{sig}^{\beta_2}(\dot{x}_2) \end{bmatrix}$.

In order to deal with the unknown upper bound of target maneuvering, an integral sliding mode three-dimensional guidance law is designed using the adaptive control as follows

$$\begin{aligned} \boldsymbol{u} &= -\boldsymbol{B}^{-1}\Big(\boldsymbol{F} + k_3\boldsymbol{s} + k_4 \mathrm{sign}(\boldsymbol{s}) + \boldsymbol{M} \\ &\quad + k_5 \frac{\boldsymbol{s}}{\|\boldsymbol{s}\|} \tanh(\hat{D})\Big) \end{aligned} \tag{15}$$

$$\dot{\hat{\Lambda}}_1 = -p_1 s_1 \int_0^t (k_1 \mathrm{sig}^{\alpha_1}(x_1) + k_2 \mathrm{sig}^{\alpha_2}(\dot{x}_1))\mathrm{d}t \tag{16}$$

$$\dot{\hat{\Lambda}}_2 = -p_2 s_2 \int_0^t (l_1 \mathrm{sig}^{\beta_1}(x_1) + l_2 \mathrm{sig}^{\beta_2}(\dot{x}_2))\mathrm{d}t \tag{17}$$

$$\dot{\hat{D}} = \frac{\gamma}{k_5} \cosh^2(\hat{D}) \|\boldsymbol{s}\| \tag{18}$$

where $k_3, k_4, k_5, \gamma, p_1$ and $p_2$ are positive constants.

*Theorem 1:* Considering system model (10) selecting the sliding modemanifold (13), under thedesigned three-dimensional guidancelaw (15), the $\boldsymbol{s}$ sconverges to zeroin finite time, then theline of sight angularrate $\dot{\theta}_L$ and $\dot{\phi}_L$ and will convergeto zero in finite time.

*Proof:* Choose the Lyapunov function candidate as

$$V_1 = \frac{1}{2}\boldsymbol{s}^{\mathrm{T}}\boldsymbol{s} + \frac{1}{2\gamma}\tilde{D}^2 \tag{19}$$

where $\tilde{D} = D - k_5 \tanh(\hat{D})$.

The time derivative of $V_1$ can be written as

$$\begin{aligned} \dot{V}_1 &= \boldsymbol{s}^{\mathrm{T}}\dot{\boldsymbol{s}} - \frac{k_5}{\gamma}\tilde{D}\frac{1}{\cosh^2(\hat{D})}\dot{\hat{D}} \\ &= \boldsymbol{s}^{\mathrm{T}}\Big(\boldsymbol{B}\boldsymbol{u} + \boldsymbol{D} + \boldsymbol{F} + \boldsymbol{M} \\ &\quad + \begin{bmatrix} \dot{\hat{\Lambda}}_1 \int_0^t (k_1 \mathrm{sig}^{\alpha_1}(x_1) + k_2 \mathrm{sig}^{\alpha_2}(\dot{x}_1))\mathrm{d}t \\ \dot{\hat{\Lambda}}_2 \int_0^t (l_1 \mathrm{sig}^{\beta_1}(x_2) + l_2 \mathrm{sig}^{\beta_2}(\dot{x}_2))\mathrm{d}t \end{bmatrix}\Big) \\ &\quad - \frac{k_5}{\gamma}\tilde{D}\frac{1}{\cosh^2(\hat{D})}\dot{\hat{D}} \end{aligned} \tag{20}$$

Substituting (15) -(18) into (20) yields

$$\begin{aligned} \dot{V}_1 &= \boldsymbol{s}^{\mathrm{T}}(-k_3\boldsymbol{s} - k_4 \mathrm{sign}(\boldsymbol{s}) \\ &\quad + \begin{bmatrix} \dot{\hat{\Lambda}}_1 \int_0^t (k_1 \mathrm{sig}^{\alpha_1}(x_1) + k_2 \mathrm{sig}^{\alpha_2}(\dot{x}_1))\mathrm{d}t \\ \dot{\hat{\Lambda}}_2 \int_0^t (l_1 \mathrm{sig}^{\beta_1}(x_2) + l_2 \mathrm{sig}^{\beta_2}(\dot{x}_2))\mathrm{d}t \end{bmatrix} \\ &\quad + \boldsymbol{D} - k_5 \frac{\boldsymbol{s}}{\|\boldsymbol{s}\|} \tanh(\hat{D})) - \frac{k_5}{\gamma}\tilde{D}\frac{1}{\cosh^2(\hat{D})}\dot{\hat{D}} \\ &\leq -k_3\boldsymbol{s}^{\mathrm{T}}\boldsymbol{s} - k_4\boldsymbol{s}^{\mathrm{T}}\mathrm{sign}(\boldsymbol{s}) + \boldsymbol{n} + D\|\boldsymbol{s}\| - k_5 \tanh(\hat{D})\|\boldsymbol{s}\| \\ &\quad - \frac{k_5}{\gamma}\tilde{D}\frac{1}{\cosh^2(\hat{D})}\dot{\hat{D}} \\ &\leq -k_3\boldsymbol{s}^{\mathrm{T}}\boldsymbol{s} - k_4\boldsymbol{s}^{\mathrm{T}}\mathrm{sign}(\boldsymbol{s}) \\ &\leq 0 \end{aligned} \tag{21}$$

where $\boldsymbol{n} = \boldsymbol{s}^{\mathrm{T}} \begin{bmatrix} \dot{\hat{\Lambda}}_1 \int_0^t (k_1 \mathrm{sig}^{\alpha_1}(x_1) + k_2 \mathrm{sig}^{\alpha_2}(\dot{x}_1))\mathrm{d}t \\ \dot{\hat{\Lambda}}_2 \int_0^t (l_1 \mathrm{sig}^{\beta_1}(x_2) + l_2 \mathrm{sig}^{\beta_2}(\dot{x}_2))\mathrm{d}t \end{bmatrix}$.

From (20), it can get that $V_1$ is bounded. Meanwhile, it can conclude that adaptive parameter estimate $\hat{D}$ is bounded, which means that there is positive constant $\bar{D} > 0$, satisfying $\hat{D} \leq \bar{D}$.

Choose the Lyapunov function candidate as

$$V_2 = \frac{1}{2}\boldsymbol{s}^{\mathrm{T}}\boldsymbol{s} + \frac{1}{\gamma}\left(\bar{D} - k_5\tanh(\hat{D})\right)^2 \tag{22}$$

where $\bar{D}$ is positive constant, satisfying $\bar{D} > \hat{D}$ and $\bar{D} > D$.

The time derivative of the $V_2$ can be written as

$$\begin{aligned}
\dot{V}_2 &= \boldsymbol{s}^{\mathrm{T}}\dot{\boldsymbol{s}} - \frac{2k_5}{\gamma}\left(\bar{D} - k_5\tanh(\hat{D})\right)\frac{1}{\cosh^2(\hat{D})}\dot{\hat{D}} \\
&= \boldsymbol{s}^{\mathrm{T}}\left(\boldsymbol{B}\boldsymbol{u} + \boldsymbol{D} + \boldsymbol{F} + \boldsymbol{M}\right. \\
&\quad \left. + \begin{bmatrix} \dot{\hat{\Lambda}}_1 \int_0^t (k_1\mathrm{sig}^{\alpha_1}(x_1) + k_2\mathrm{sig}^{\alpha_2}(\dot{x}_1))\mathrm{d}t \\ \dot{\hat{\Lambda}}_2 \int_0^t (l_1\mathrm{sig}^{\beta_1}(x_2) + l_2\mathrm{sig}^{\beta_2}(\dot{x}_2))\mathrm{d}t \end{bmatrix}\right) \\
&\quad - \frac{2k_5}{\gamma}\left(\bar{D} - k_5\tanh(\hat{D})\right)\frac{1}{\cosh^2(\hat{D})}\dot{\hat{D}} \\
&= -k_3\boldsymbol{s}^{\mathrm{T}}\boldsymbol{s} - k_4\boldsymbol{s}^{\mathrm{T}}\mathrm{sign}(\boldsymbol{s}) + \boldsymbol{n} + \boldsymbol{D} - k_5\frac{\boldsymbol{s}}{\|\boldsymbol{s}\|}\tanh(\hat{D})) \\
&\quad - \frac{2k_5}{\gamma}\left(\bar{D} - k_5\tanh(\hat{D})\right)\frac{1}{\cosh^2(\hat{D})}\dot{\hat{D}} \\
&\le -k_3\boldsymbol{s}^{\mathrm{T}}\boldsymbol{s} - k_4\boldsymbol{s}^{\mathrm{T}}\mathrm{sign}(\boldsymbol{s}) + \bar{D}\|\boldsymbol{s}\| - k_5\tanh(\hat{D}) \\
&\quad - \begin{bmatrix} p_1 s_1^2\left(\int_0^t (k_1\mathrm{sig}^{\alpha_1}(x_1) + k_2\mathrm{sig}^{\alpha_2}(\dot{x}_1))\mathrm{d}t\right)^2 \\ p_1 s_2^2\left(\int_0^t (l_1\mathrm{sig}^{\beta_1}(x_2) + l_2\mathrm{sig}^{\beta_2}(\dot{x}_2))\mathrm{d}t\right)^2 \end{bmatrix} \\
&\quad - \frac{2k_5}{\gamma}\left(\bar{D} - k_4\tanh(\hat{D})\right)\frac{1}{\cosh^2(\hat{D})}\dot{\hat{D}} \\
&\le -k_4\|\boldsymbol{s}\| - \left(\bar{D} - k_5\tanh(\hat{D})\right)\|\boldsymbol{s}\| \\
&\le -\rho V_2^{1/2}
\end{aligned} \tag{23}$$

where $\rho = \min(\sqrt{2}k_4, \sqrt{\gamma}\|s\|)$. Considering (23) and Lemma1, it can conclude that the sliding mode manifold $\boldsymbol{s}$ converges to zero in finite time.

According to (13), the inequality is satisfied

$$\begin{aligned}
\ddot{x}_1 &= -\dot{\hat{\Lambda}}_1\int_0^t (k_1\mathrm{sig}^{\alpha_1}(x_1) + k_2\mathrm{sig}^{\alpha_2}(\dot{x}_1))\mathrm{d}t \\
&\quad - k_1\hat{\Lambda}_1\mathrm{sig}^{\alpha_1}(x_1) - k_2\hat{\Lambda}_1\mathrm{sig}^{\alpha_2}(\dot{x}_1) \\
\ddot{x}_2 &= -\dot{\hat{\Lambda}}_2\int_0^t (l_1\mathrm{sig}^{\beta_1}(x_2) + l_2\mathrm{sig}^{\beta_2}(\dot{x}_2))\mathrm{d}t - l_1\hat{\Lambda}_2\mathrm{sig}^{\beta_1}(x_2) \\
&\quad - l_2\hat{\Lambda}_2\mathrm{sig}^{\beta_2}(\dot{x}_2)
\end{aligned} \tag{24}$$

As can be seen from the [9], $x_1$ and $x_2$ converges to zero in finite time, that is, the line of sight angular rate $\dot{\theta}_L$ and $\dot{\phi}_L$ will converge to zero in finite time.

Theorem 1 is proved.

*Remark 1:* In the guidance law (15), the design constraints of the guidance law are not considered, but in the actual guidance process, only the aerodynamic force provides maneuverability for the missile in the final guidance stage, which leads to the fact that the power actuator of the missile can only provide limited acceleration. So it is of great significance to design the guidance law with acceleration saturation.

### B. DESIGN OF ANTI-SATURATION ADAPTIVE INTEGRAL SLIDING MODE CONTROLLER

Considering the input saturation, the (10) can be rewritten as

$$\ddot{\boldsymbol{x}} = \boldsymbol{F} + \boldsymbol{B}\mathrm{sat}(\boldsymbol{u}) + \boldsymbol{D} \tag{25}$$

In order to cope with input saturation, the auxiliary system (26) is introduced, as shown at the bottom of the page, where $\Delta\boldsymbol{u} = \boldsymbol{u} - \boldsymbol{u}_c$, $\boldsymbol{u}_c$ is the actual control input, $\boldsymbol{\eta}$ is the state of the auxiliary system, $\sigma, k_\eta, k_{\eta 1}$ and $\gamma_1$ are positive constants, $0 < \gamma_1 < 1$.

An adaptive anti-saturation three dimensional guidance law is designed as

$$\begin{aligned}
\boldsymbol{u}_c &= -\boldsymbol{B}^{-1}\left(\boldsymbol{F} + k_3\boldsymbol{s} + k_4\mathrm{sign}(\boldsymbol{s}) + \boldsymbol{M}\right. \\
&\quad \left. + k_5\frac{\boldsymbol{s}}{\|\boldsymbol{s}\|}\tanh(\hat{D}) - k_\eta\boldsymbol{\eta}\right)
\end{aligned} \tag{27}$$

$$\dot{\hat{\Lambda}}_1 = -p_1 s_1\int_0^t (k_1\mathrm{sig}^{\alpha_1}(x_1) + k_2\mathrm{sig}^{\alpha_2}(\dot{x}_1))\mathrm{d}t \tag{28}$$

$$\dot{\hat{\Lambda}}_2 = -p_2 s_2\int_0^t (l_1\mathrm{sig}^{\beta_1}(x_1) + l_2\mathrm{sig}^{\beta_2}(\dot{x}_2))\mathrm{d}t \tag{29}$$

$$\dot{\hat{D}} = \frac{\gamma}{k_5}\cosh^2(\hat{D})\|s\| \tag{30}$$

*Theorem 2:* Considering the system model (10) sujecting to input saturation, selecting the sliding mode surface (14), and under the adaptive anti-saturation integral sliding mode guidance law (27), the line of sight angular rate $\dot{\theta}_L$ and $\dot{\phi}_L$ converge to zero in finite time.

*Proof :* Choose the Lyapunov function $V_3$ as

$$V_3 = \frac{1}{2}\boldsymbol{s}^{\mathrm{T}}\boldsymbol{s} + \frac{1}{2}\boldsymbol{\eta}^{\mathrm{T}}\boldsymbol{\eta} + \frac{1}{2\gamma}\tilde{D}^2 \tag{31}$$

Applying (27), the time derivative of $V_3$ can be written as

$$\begin{aligned}
\dot{V}_3 &= \boldsymbol{s}^{\mathrm{T}}\dot{\boldsymbol{s}} + \boldsymbol{\eta}^{\mathrm{T}}\dot{\boldsymbol{\eta}} + \frac{1}{\gamma}\tilde{D}\dot{\tilde{D}} \\
&= \boldsymbol{s}^{\mathrm{T}}\left(\begin{array}{l}\boldsymbol{B}\mathrm{sat}(\boldsymbol{u}) + \boldsymbol{D} + \boldsymbol{F} + \boldsymbol{M} \\ + \begin{bmatrix} \dot{\hat{\Lambda}}_1 \int_0^t (k_1\mathrm{sig}^{\alpha_1}(x_1) + k_2\mathrm{sig}^{\alpha_2}(\dot{x}_1))\mathrm{d}t \\ \dot{\hat{\Lambda}}_2 \int_0^t (l_1\mathrm{sig}^{\beta_1}(x_2) + l_2\mathrm{sig}^{\beta_2}(\dot{x}_2))\mathrm{d}t \end{bmatrix}\end{array}\right) \\
&\quad + \boldsymbol{\eta}^{\mathrm{T}}\dot{\boldsymbol{\eta}} - \frac{k_5}{\gamma}\tilde{D}\frac{1}{\cosh^2(\hat{D})}\dot{\hat{D}}
\end{aligned}$$

$$\dot{\boldsymbol{\eta}} = \begin{cases} -k_\eta\boldsymbol{\eta} - \dfrac{\boldsymbol{\eta}}{\|\boldsymbol{\eta}\|^2}\left(\left|\boldsymbol{s}^{\mathrm{T}}\boldsymbol{B}_1\Delta\boldsymbol{u}\right| + \dfrac{1}{2}\Delta\boldsymbol{u}^{\mathrm{T}}\Delta\boldsymbol{u}\right) + \Delta\boldsymbol{u} - k_{\eta 1}\mathrm{sig}(\boldsymbol{\eta})^{\gamma_1}, & \|\boldsymbol{\eta}\| \ge \sigma \\ 0, & \|\boldsymbol{\eta}\| < \sigma \end{cases} \tag{26}$$

$$= \boldsymbol{s}^{\mathrm{T}}(-k_3\boldsymbol{s} - k_4\mathrm{sign}(\boldsymbol{s}) + \boldsymbol{D} - k_5\frac{\boldsymbol{s}}{\|\boldsymbol{s}\|}\tanh(\hat{D})) + \boldsymbol{n} + \boldsymbol{s}^{\mathrm{T}}\boldsymbol{B}\Delta\boldsymbol{u} + k_\eta\boldsymbol{s}^{\mathrm{T}}\boldsymbol{\eta} + \boldsymbol{\eta}^{\mathrm{T}}\dot{\boldsymbol{\eta}} - \frac{k_5}{\gamma}\tilde{D}\frac{1}{\cosh^2(\hat{D})}\dot{\hat{D}}$$
$$\leq \boldsymbol{s}^{\mathrm{T}}(-k_3\boldsymbol{s} - k_4\mathrm{sign}(\boldsymbol{s}) + \boldsymbol{D} - k_5\frac{\boldsymbol{s}}{\|\boldsymbol{s}\|}\tanh(\hat{D})) + \boldsymbol{n} + k_\eta\boldsymbol{s}^{\mathrm{T}}\boldsymbol{\eta} - k_\eta\boldsymbol{\eta}^{\mathrm{T}}\boldsymbol{\eta} - \left(\left|\boldsymbol{s}^{\mathrm{T}}\boldsymbol{B}\Delta\boldsymbol{u}\right| + \frac{1}{2}\Delta\boldsymbol{u}^{\mathrm{T}}\Delta\boldsymbol{u}\right) + \boldsymbol{\eta}^{\mathrm{T}}\Delta\boldsymbol{u} - k_{\eta 1}\boldsymbol{\eta}^{\mathrm{T}}\mathrm{sig}(\boldsymbol{\eta})^{\gamma} - \frac{k_5}{\gamma}\tilde{D}\frac{1}{\cosh^2(\hat{D})}\dot{\hat{D}} \quad (32)$$

As

$$\boldsymbol{s}^{\mathrm{T}}\boldsymbol{B}\Delta\boldsymbol{u} - \left|\boldsymbol{s}^{\mathrm{T}}\boldsymbol{B}\Delta\boldsymbol{u}\right| \leq 0 \quad (33)$$

$$k_\eta\boldsymbol{s}^{\mathrm{T}}\boldsymbol{\eta} + \boldsymbol{\eta}^{\mathrm{T}}\Delta\boldsymbol{u} \leq \frac{1}{2}k_\eta\boldsymbol{s}^{\mathrm{T}}\boldsymbol{s} + \frac{1}{2}\left(k_\eta + 1\right)\boldsymbol{\eta}^{\mathrm{T}}\boldsymbol{\eta} + \frac{1}{2}\Delta\boldsymbol{u}^{\mathrm{T}}\Delta\boldsymbol{u} \quad (34)$$

According to (33) and (34), then (32) can be rewritten as

$$\dot{V}_2 \leq -k_3\boldsymbol{s}^{\mathrm{T}}\boldsymbol{s} - k_4\boldsymbol{s}^{\mathrm{T}}\mathrm{sign}(\boldsymbol{s}) - \left(k_\eta - \frac{1}{2}\left(k_\eta + 1\right)\right)\boldsymbol{\eta}^{\mathrm{T}}\boldsymbol{\eta} - k_{\eta 1}\boldsymbol{\eta}^{\mathrm{T}}\mathrm{sig}(\boldsymbol{\eta})^{\gamma_1} + D\|\boldsymbol{s}\| - k_5\tanh(\hat{D})\|\boldsymbol{s}\| - \frac{k_5}{\gamma}\tilde{D}\frac{1}{\cosh^2(\hat{D})}\dot{\hat{D}}$$
$$\leq -k_3\boldsymbol{s}^{\mathrm{T}}\boldsymbol{s} - k_4\boldsymbol{s}^{\mathrm{T}}\mathrm{sign}(\boldsymbol{s}) - \left(k_\eta - \frac{1}{2}\left(k_\eta + 1\right)\right)\boldsymbol{\eta}^{\mathrm{T}}\boldsymbol{\eta} - k_{\eta 1}\boldsymbol{\eta}^{\mathrm{T}}\mathrm{sig}(\boldsymbol{\eta})^{\gamma_1} + \tilde{D}\|\boldsymbol{s}\| - \frac{k_5}{\gamma}\tilde{D}\frac{1}{\cosh^2(\hat{D})}\dot{\hat{D}}$$
$$\leq -k_4\boldsymbol{s}^{\mathrm{T}}\mathrm{sign}(\boldsymbol{s}) - \frac{1}{2}\left(k_\eta + 1\right)\boldsymbol{\eta}^{\mathrm{T}}\boldsymbol{\eta} - k_{\eta 1}\boldsymbol{\eta}^{\mathrm{T}}\mathrm{sig}(\boldsymbol{\eta})^{\gamma_1} - k_3\boldsymbol{s}^{\mathrm{T}}\boldsymbol{s}$$
$$\leq 0 \quad (35)$$

From (35), it can get that $V_3$ is bounded. Meanwhile, it can conclude that $\hat{D}$ is bounded, which means the existence of positive constant $\bar{D} > 0$, satisfying $\hat{D} \leq \bar{D}$.

*Proof :* Choose the Lyapunov function candidate as

$$V_4 = \frac{1}{2}\boldsymbol{s}^{\mathrm{T}}\boldsymbol{s} + \frac{1}{2}\boldsymbol{\eta}^{\mathrm{T}}\boldsymbol{\eta} + \frac{1}{\gamma}\left(\bar{D} - k_5\tanh(\hat{D})\right)^2 \quad (36)$$

Applying (27), the time derivative of (36)can be written as

$$\dot{V}_4 = \boldsymbol{s}^{\mathrm{T}}\left(\begin{array}{l}\boldsymbol{B}\mathrm{sat}(\boldsymbol{u}) + \boldsymbol{D} + \boldsymbol{F} + \boldsymbol{M} \\ + \left[\begin{array}{l}\dot{\hat{\Lambda}}_1\int_0^t\left(k_1\mathrm{sig}^{\alpha_1}(x_1) + k_2\mathrm{sig}^{\alpha_2}(\dot{x}_1)\right)\mathrm{d}t \\ \dot{\hat{\Lambda}}_2\int_0^t\left(l_1\mathrm{sig}^{\beta_1}(x_2) + l_2\mathrm{sig}^{\beta_2}(\dot{x}_2)\right)\mathrm{d}t\end{array}\right]\end{array}\right) + \boldsymbol{\eta}^{\mathrm{T}}\dot{\boldsymbol{\eta}} - \frac{2k_5}{\gamma}\left(\bar{D} - k_5\tanh(\hat{D})\right)\frac{1}{\cosh^2(\hat{D})}\dot{\hat{D}}$$
$$= \boldsymbol{s}^{\mathrm{T}}(-k_3\boldsymbol{s} - k_4\mathrm{sign}(\boldsymbol{s}) + \boldsymbol{D} - k_5\frac{\boldsymbol{s}}{\|\boldsymbol{s}\|}\tanh(\hat{D})) + \boldsymbol{n} + \boldsymbol{s}^{\mathrm{T}}\boldsymbol{B}\Delta\boldsymbol{u} + k_\eta\boldsymbol{s}^{\mathrm{T}}\boldsymbol{\eta} + \boldsymbol{\eta}^{\mathrm{T}}\dot{\boldsymbol{\eta}} - \frac{2k_5}{\gamma}\left(\bar{D} - k_4\tanh(\hat{D})\right)\frac{1}{\cosh^2(\hat{D})}\dot{\hat{D}}$$
$$\leq \boldsymbol{s}^{\mathrm{T}}(-k_3\boldsymbol{s} - k_4\mathrm{sign}(\boldsymbol{s}) + \boldsymbol{n} + \boldsymbol{D} - k_5\frac{\boldsymbol{s}}{\|\boldsymbol{s}\|}\tanh(\hat{D})) - k_\eta\boldsymbol{\eta}^{\mathrm{T}}\boldsymbol{\eta} - \left(\left|\boldsymbol{s}^{\mathrm{T}}\boldsymbol{B}\Delta\boldsymbol{u}\right| + \frac{1}{2}\Delta\boldsymbol{u}^{\mathrm{T}}\Delta\boldsymbol{u}\right) + \boldsymbol{\eta}^{\mathrm{T}}\Delta\boldsymbol{u} - k_{\eta 1}\boldsymbol{\eta}^{\mathrm{T}}\mathrm{sig}(\boldsymbol{\eta})^{\gamma} - \frac{2k_5}{\gamma}\left(\bar{D} - k_5\tanh(\hat{D})\right)\frac{1}{\cosh^2(\hat{D})}\dot{\hat{D}} \quad (37)$$

According to (33) and (34), (37) can be rewritten as

$$\dot{V}_4 \leq -k_3\boldsymbol{s}^{\mathrm{T}}\boldsymbol{s} - k_4\boldsymbol{s}^{\mathrm{T}}\mathrm{sign}(\boldsymbol{s}) - \left(k_\eta - \frac{1}{2}\left(k_{\eta 1} + 1\right)\right)\boldsymbol{\eta}^{\mathrm{T}}\boldsymbol{\eta} - k_{\eta 1}\boldsymbol{\eta}^{\mathrm{T}}\mathrm{sig}(\boldsymbol{\eta})^{\gamma_1} + \boldsymbol{n} + \boldsymbol{s}^{\mathrm{T}}(\boldsymbol{D} - k_5\frac{\boldsymbol{s}}{\|\boldsymbol{s}\|}\tanh(\hat{D})) - \frac{2k_5}{\gamma}\left(\bar{D} - k_5\tanh(\hat{D})\right)\frac{1}{\cosh^2(\hat{D})}\dot{\hat{D}}$$
$$\leq -k_3\boldsymbol{s}^{\mathrm{T}}\boldsymbol{s} - k_4\boldsymbol{s}^{\mathrm{T}}\mathrm{sign}(\boldsymbol{s}) - \frac{1}{2}\left(k_\eta - 1\right)\boldsymbol{\eta}^{\mathrm{T}}\boldsymbol{\eta} - k_{\eta 1}\boldsymbol{\eta}^{\mathrm{T}}\mathrm{sig}(\boldsymbol{\eta})^{\gamma_1} + \bar{D}\|\boldsymbol{s}\| - k_5\tanh(\hat{D})\|\boldsymbol{s}\| - \frac{2k_5}{\gamma}\left(\bar{D} - k_4\tanh(\hat{D})\right)\frac{1}{\cosh^2(\hat{D})}\dot{\hat{D}}$$
$$\leq -k_3\boldsymbol{s}^{\mathrm{T}}\boldsymbol{s} - k_4\boldsymbol{s}^{\mathrm{T}}\mathrm{sign}(\boldsymbol{s}) - \frac{1}{2}\left(k_\eta - 1\right)\boldsymbol{\eta}^{\mathrm{T}}\boldsymbol{\eta} - k_{\eta 1}\boldsymbol{\eta}^{\mathrm{T}}\mathrm{sig}(\boldsymbol{\eta})^{\gamma_1} - \left(\bar{D} - k_5\tanh(\hat{D})\right)\|\boldsymbol{s}\|$$
$$\leq -k_4\boldsymbol{s}^{\mathrm{T}}\mathrm{sign}(\boldsymbol{s}) - k_{\eta 1}\boldsymbol{\eta}^{\mathrm{T}}\mathrm{sig}(\boldsymbol{\eta})^{\gamma_1} - \left(\bar{D} - k_5\tanh(\hat{D})\right)\|\boldsymbol{s}\|$$
$$\leq -\min\left(\sqrt{2}k_4, 2^{\frac{\gamma_1+1}{2}}k_{\eta 1}, \sqrt{\gamma}, \|\boldsymbol{s}\|\right)\min\left(V_4^{1/2}, V_4^{(\gamma+1)/2}\right) \quad (38)$$

From (38) and lemma1, it can be seen the sliding mode manifold $\boldsymbol{s}$ can converge to zero.

## IV. SIMULATION RESULTS

In order to show the effectiveness of the designed guidance law, the simulation parameters is given in Table 1.

### A. SIMULATION ANALYSIS OF ADAPTIVE INTEGRAL SLIDING MODE GUIDANCE LAW

In order to verify the effectiveness of the adaptive integral sliding mode guidance law (15), compared with the guidance law NTSMGL in reference [14] and external disturbances are considered as $\boldsymbol{D} = \begin{bmatrix}\frac{\cos\theta_t}{R}a_{zt} \\ \frac{\cos\phi_t}{R\cos\theta_L}a_{yt} - \frac{\sin\theta_t\sin\phi_t}{R\cos\theta_L}a_{zt}\end{bmatrix}$. The parameters of the observer are selected as: $k_1 = 0.25$, $k_2 = 0.2$, $k_3 = 0.5$, $k_4 = 0.3$, $k_5 = 1.5$, $\gamma = 0.7$, $l_1 = 0.5$, $l_2 = 0.5$, $\alpha_1 = 0.6$, $\alpha_2 = 0.65$, $\beta_1 = 0.75$, $\beta_2 = 0.75$, $p_1 = 0.02$, $p_2 = 0.02$. The maximum acceleration of the missile is $u_m = 25g$. The simulation results are shown in fig. 2.

**TABLE 1. Initial engagement parameters for the missile and target.**

| parameters | initial values | parameters | initial values |
|---|---|---|---|
| $R(0)$(m) | 5000 | $V_m$(m/ $s$) | 800 |
| $\theta_L(0)$(deg) | 5 | $\theta_t(0)$(deg) | 20 |
| $\phi_L(0)$(deg) | 5 | $\phi_t(0)$(deg) | 20 |
| $\theta_m(0)$(deg) | 20 | $V_t$(m/ $s$) | 500 |
| $\phi_m(0)$(deg) | 20 | | |

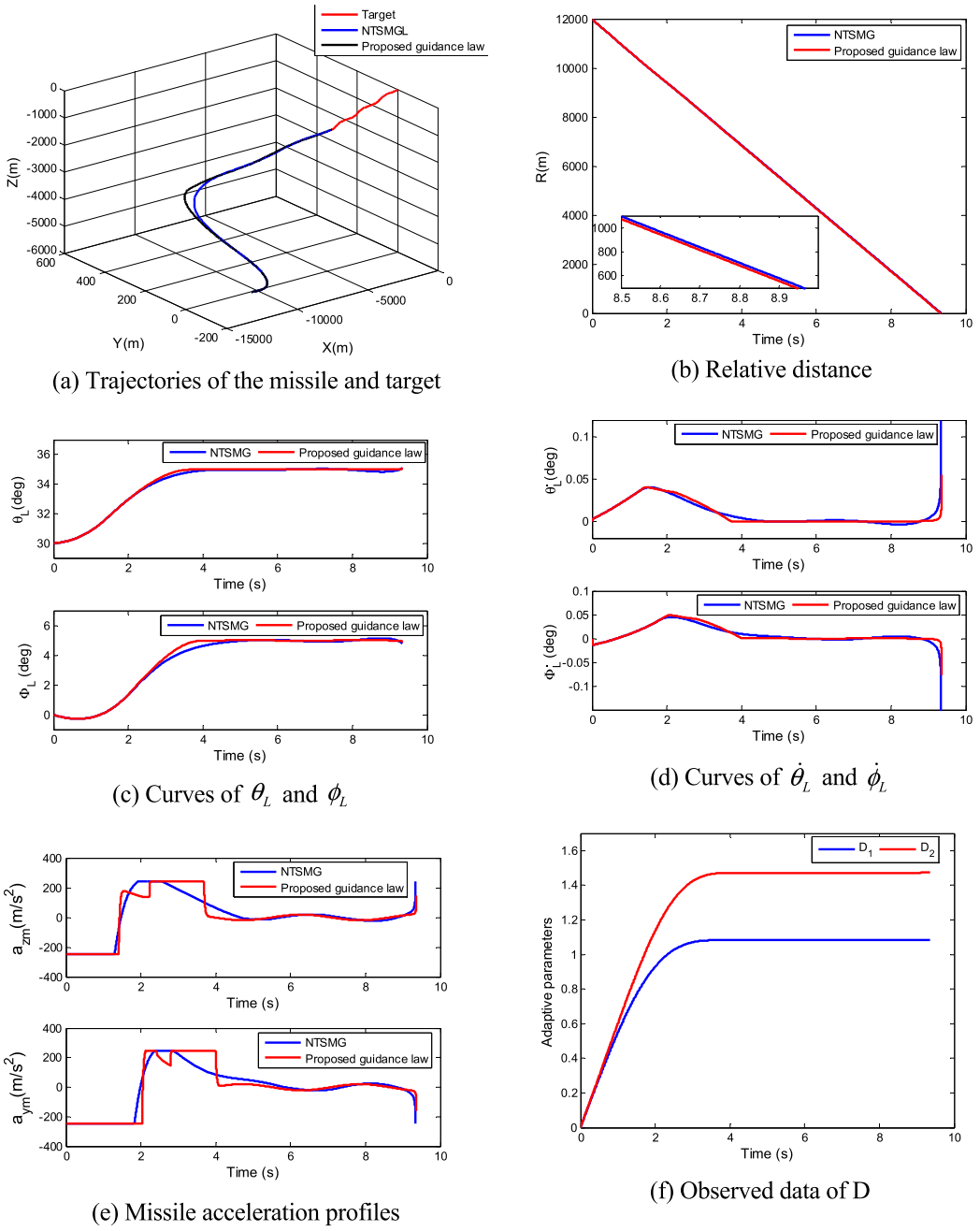


(a) Trajectories of the missile and target

(b) Relative distance

(c) Curves of $\theta_L$ and $\phi_L$

(d) Curves of $\dot{\theta}_L$ and $\dot{\phi}_L$

(e) Missile acceleration profiles

(f) Observed data of D

**FIGURE 2. Simulation results under guidance law(15).**

The trajectory and relative distance curve of missile and target under the NTSMG and proposed guidance law are given in Fig.2 a)-(b), respectively. it can be seen that these two guidance laws can intercept the target successfully. Fig.2(c)-(d) gives the curves of $\dot{\theta}_L$ and $\dot{\phi}_L$ of line-of-sight angular rate respectively. It can be seen from the simulation result that the line-of-sight angular rate $\dot{\theta}_L$ and $\dot{\phi}_L$ can converge to zero fast under the two kinds of guidance laws, and have faster convergence rate and higher convergence accuracy than the NTSMG. From the acceleration curve of the missile given in Fig.2(e), it can be seen that the acceleration saturation phenomenon of the guidance law designed in this paper and tends to be stable value after a period of time compared with that of NTSMG. From the adaptive parameter curve given in Fig.2(f), it can be seen that it can tend to a steady state in a short time, which shows that the adaptive law is effective in the guidance process.

### *B. SIMULATION ANALYSIS OF ANTI-SATURATION ADAPTIVE SLIDING MODE GUIDANCE LAW*

In order to demonstrate the effectiveness of theanti-saturation adaptive slidingmode guidance law (27), the following two forms of target maneuvering are simulated and analyzed.

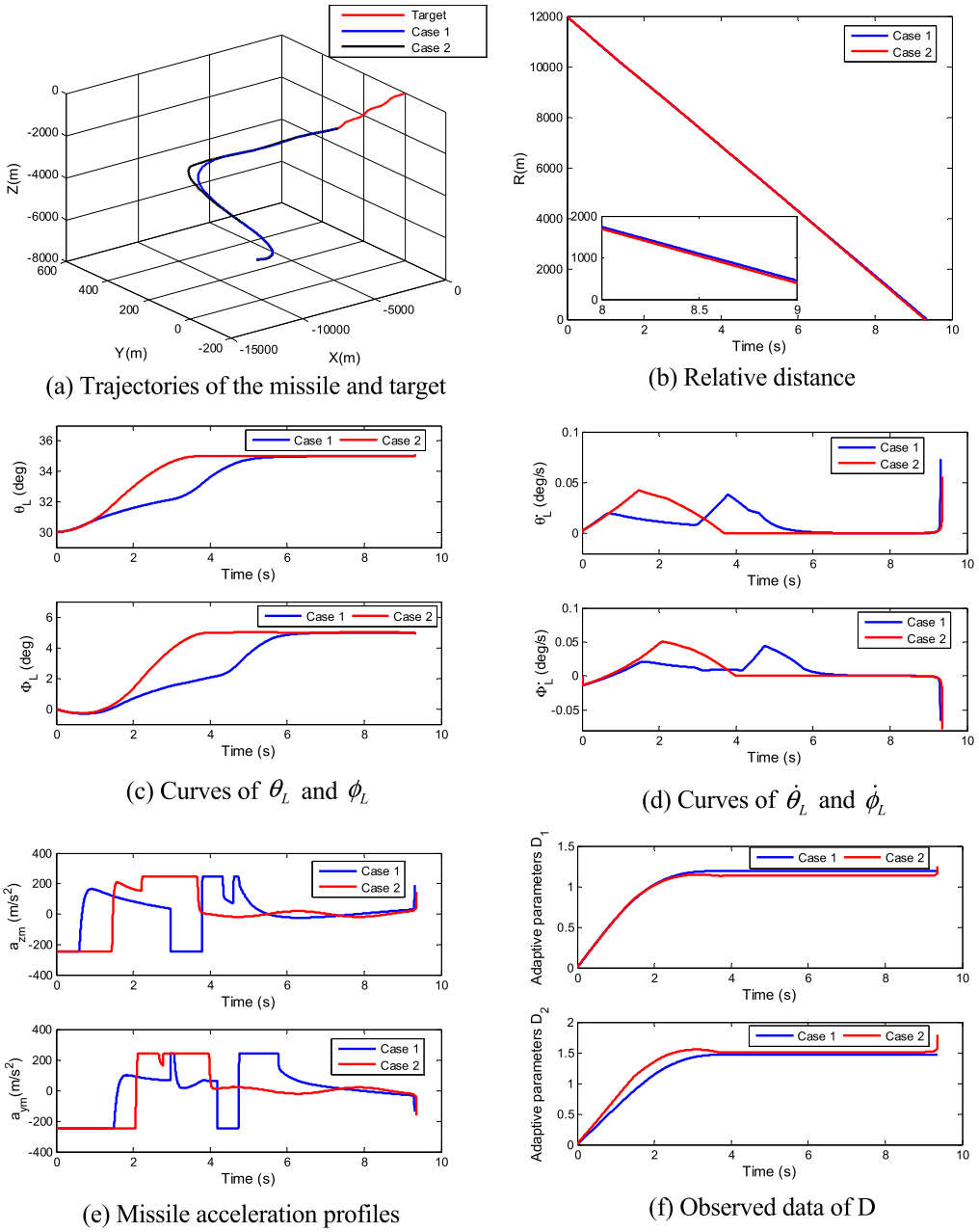


(a) Trajectories of the missile and target

(b) Relative distance

(c) Curves of $\theta_L$ and $\phi_L$

(d) Curves of $\dot{\theta}_L$ and $\dot{\phi}_L$

(e) Missile acceleration profiles

(f) Observed data of D

**FIGURE 3.** Simulation results under guidance law(27).

Case1 : $a_{zt} = a_{yt} = 8$ m/s$^2$

Case2 : $a_{yt} = a_{zt} = 8\cos(4t)$ m/s$^2$

The guidance law parameters are chosen as: $\sigma = 0.01$, $k_\eta = 1.25$, $k_{\eta 1} = 0.5$ and $\gamma_1 = 0.72$, other guidance parameters are the same as in section 4.1, the simulation results are shown in Fig. 3.

Fig.3 (a)-(b) gives the trajectory curve and relative distance curve of missile and target under two forms of target maneuverability. It can be seen that the missile can accurately intercept the target and satisfy the guidance accuracy. Fig.3(c)-(d) show the curves of $\dot{\theta}_L$ and $\dot{\phi}_L$ of line-of-sight angular rate, which can fast converge to zero in finite time, and that ensures that the missile can hit the target accurately. From the curve of missile acceleration given in Fig.3 (e), it can be seen that after a period of time, the the acceleration curve tends to be steady value, and the control amplitude is always within the constraint range in the whole control process, which satisfies the input constraint. From the adaptive parameter curve given in Fig.3 (f), it can be seen that the adaptive estimation value can tend to a steady state value in a short time.

## V. CONCLUSION

In this paper, a three-dimensional guidance scheme with impact angle constraints and input saturation is designed for

intercepting maneuvering targets. The main results are as follows:

(1) An adaptive algorithm is introduced to estimate the upper bound of the maneuvering acceleration of the target, which relaxes the requirement of the prior information of the maneuvering acceleration of the target.

(2) The adaptive three-dimensional guidance law and anti-saturation three-dimensional guidance law are designed based on the integral terminal sliding mode control, respectively, which can ensure that the line of sight angular rate converges to zero in finite time.

(3) The system state is proved to be finite time stable under the designed guidance strategy by using Lyapunov theory, and the effectiveness of the guidance scheme is verified by digital simulation.

## REFERENCES


[1] G. Li and Y. Wu, "Nonsingular adaptive-gain super-twisting guidance with an impact angle constraint," *Proc. Inst. Mech. Eng., G, J. Aerosp. Eng.*, vol. 233, no. 5, pp. 1705–1714, Apr. 2019.

[2] X. B. Li, G. R. Zhao, S. Liu, and X. Han, "Adaptive integral sliding mode guidance law with impact angle constraint considering autopilot lag," *J. Phys., Conf. Ser.*, vol. 1267, Jul. 2019, Art. no. 012081.

[3] K. S. Erer and O. Merttopçuoglu, "Indirect impact-angle-control against stationary targets using biased pure proportional navigation," *J. Guid., Control, Dyn.*, vol. 35, no. 2, pp. 700–704, Mar. 2012.

[4] C.-H. Lee, T.-H. Kim, and M.-J. Tahk, "Interception angle control guidance using proportional navigation with error feedback," *J. Guid., Control, Dyn.*, vol. 36, no. 5, pp. 1556–1561, Sep. 2013.

[5] S. K. Pandit, B. Panchal, and S. E. Talole, "Design of 3D guidance law for tactical missiles," *Proc. Int. Conf. Modern Res. Aerosp. Eng.* Singapore: Springer, 2018, pp. 61–68.

[6] W. Pang, X. Xie, and T. Sun, "Improved bias proportional navigation with multiple constraints for guide ammunition," *J. Syst. Eng. Electron.*, vol. 2017, vol. 28, no. 6, pp. 1193–1202.

[7] B.-G. Park, T.-H. Kim, and M.-J. Tahk, "Range-to-go weighted optimal guidance with impact angle constraint and seeker's look angle limits," *IEEE Trans. Aerosp. Electron. Syst.*, vol. 52, no. 3, pp. 1241–1256, Jun. 2016.

[8] X. Chen and J. Wang, "Optimal control based guidance law to control both impact time and impact angle," *Aerosp. Sci. Technol.*, vol. 84, pp. 454–463, Jan. 2019.

[9] J. G. Sun, S. M. Song, and H. T. Chen, "Finite-time tracking control of hypersonic aircrafts with input saturation," *Proc. Inst. Mech. Eng. G, J. Aerosp. Eng.*, vol. 232, no. 7, pp. 1373–1389, 2018.

[10] H. Sun, S. Li, and C. Sun, "Finite time integral sliding mode control of hypersonic vehicles," *Nonlinear Dyn.*, vol. 73, nos. 1–2, pp. 229–244, Jul. 2013.

[11] V. I. Utkin and H. C. Chang, "Sliding mode control on electro-mechanical systems," *Math. Problems Eng.*, vol. 8, no. 4, pp. 451–473, 2002.

[12] S. Lyu, Z. H. Zhu, S. Tang, and X. Yan, "Fast nonsingular terminal sliding mode to attenuate the chattering for missile interception with finite time convergence," *IFAC-PapersOnLine*, vol. 49, no. 17, pp. 34–39, 2016.

[13] Y. Si and S. Song, "Three-dimensional adaptive finite-time guidance law for intercepting maneuvering targets," *Chin. J. Aeronaut.*, vol. 30, no. 6, pp. 1985–2003, Dec. 2017.

[14] S. R. Kumar and D. Ghose, "Three-dimensional impact angle guidance with coupled engagement dynamics," *Proc. Inst. Mech. Eng. G, J. Aerosp. Eng.*, vol. 231, no. 4, pp. 621–641, Mar. 2017.

[15] S. He and D. Lin, "Adaptive nonsingular sliding mode based guidance law with terminal angular constraint," *Int. J. Aeronaut. Space Sci.*, vol. 15, no. 2, pp. 146–152, Jun. 2014.

[16] Z. Zhang, C. Man, S. Li, and S. Jin, "Finite-time guidance laws for three-dimensional missile-target interception," *Proc. Inst. Mech. Eng. G, J. Aerosp. Eng.*, vol. 230, no. 2, pp. 392–403, Feb. 2016.

[17] J.-P. Dong, J.-G. Sun, Y. Guo, and S.-M. Song, "Guidance laws against towed decoy based on adaptive back-stepping sliding mode and anti-saturation methods," *Int. J. Control, Autom. Syst.*, vol. 16, no. 4, pp. 1724–1735, Aug. 2018.

[18] G. Hexner and A. W. Pila, "Practical stochastic optimal guidance law for bounded acceleration missiles," *J. Guid., Control, Dyn.*, vol. 34, no. 2, pp. 437–445, Mar. 2011.

[19] D. Zhou and B. Xu, "Adaptive dynamic surface guidance law with input saturation constraint and autopilot dynamics," *J. Guid., Control, Dyn.*, vol. 39, no. 5, pp. 1–8, 2016.

[20] W. Wang, S. Xiong, S. Wang, S. Song, and C. Lai, "Three dimensional impact angle constrained integrated guidance and control for missiles with input saturation and actuator failure," *Aerosp. Sci. Technol.*, vol. 53, pp. 169–187, Jun. 2016.

[21] X. L. Liang, M. Z. Hou, and G. R. Duan, "Adaptive dynamic surface control for integrated missile guidance and autopilot in the presence of input saturation," *J. Aerosp. Eng.*, vol. 28, no. 5, pp. 1–8, 2015.

[22] D. Zhou and B. Xu, "Adaptive dynamic surface guidance law with input saturation constraint and autopilot dynamics," *J. Guid., Control, Dyn.*, vol. 39, no. 5, pp. 1155–1162, May 2016.

[23] B. Xu and D. Zhou, "Three dimensional adaptive dynamic surface guidance law accounting for autopilot lag," in *Proc. Amer. Control Conf.*, Jun. 2014, pp. 578–583.


**TONG LI** received the M.E. degree in automation from Harbin Engineering University, Harbin, China, in 2015. He is currently pursuing the Ph.D. degree in engineering. His current research interest includes navigation guidance and control.

**HUAMING QIAN** is currently a Professor with the College of Automation, Harbin Engineering University. His current research interests include sensor technology and intelligent systems, and integrated navigation technology.